Combined FFT and Wavelet Analysis of Schlieren and Flame Luminosity Time-Series to Visualize Regions of Combustion Instability

SAUMYA VILAS ROY[1]*, DEEPAK MISHRA[1], RAJESH SADANANDAN[2]

[1]Department of Avionics, Indian Institute of Space Science and Technology (IIST), Thiruvananthapuram, Kerala - 695547, India
[2]Department of Aerospace Engineering, Indian Institute of Space Science and Technology (IIST), Thiruvananthapuram, Kerala - 695547, India
*Corresponding author: e-mail: rajeshsadanandan@iist.ac.in

Keywords: combustion instability, digital image processing, FFT, wavelet transform.

Abstract:
The paper reports on applying 2D digital image processing techniques to high-speed image sequences from optical diagnostic methods employed in combustion environments. The methodology involves a combined Fourier and Wavelet-based analysis of high-speed flame luminosity and Schlieren image sequences to gain insight into the spatial distribution of flame or flow density oscillations during combustion instabilities. A novel algorithm and a Python-based code are developed for this purpose. The methodology involves the computation of local intensity oscillations, spatial dominant frequency, and amplitude estimation using FFT. The temporal periodic behavior at any area of interest in this image is then obtained through wavelet-based analysis of the temporal intensity oscillation. Finally, the methodology is demonstrated for two cases of naturally excited acoustic instability occurring in a non-premixed and swirl-stabilized combustor, revealing the temporal characteristics of the frequency components present at the region of interest.

1. INTRODUCTION

Problems with combustion instabilities are present in most practical combustor systems like gas turbines, rocket propulsion systems, power generation systems, etc [1]. They are usually called self-sustained, large amplitude oscillations of pressure and velocity occurring in reacting flows. One of the causes of this phenomenon is the coupling of the acoustic characteristics of the combustor and the oscillations in the heat release rate by flame under favorable conditions. These acoustic oscillations can induce flow velocity fluctuations inside the combustor, which can, in turn, trigger hydrodynamic instabilities or vorticity fluctuations, which are spatially distributed [2]. The instabilities move along the flame, leading to flame wrinkling and heat release oscillations, thereby driving thermo-acoustic feedback. Therefore, information about the flow regions associated with oscillation is valuable in understanding the coupling between the acoustic and heat release oscillations [3].

In the present study, digital image processing techniques are employed to image series from two optical (line-of-sight) diagnostic techniques - high-speed Schlieren and high-speed flame luminosity – to capture the frequency of the corresponding spatially distributed oscillations. A novel algorithm is developed for this purpose, and a Python-based code is written to implement the methodology. The following section explains the different modules involved in the image post-processing procedure. The method is then applied to experimental data taken from non-premixed and swirl-stabilized burners undergoing acoustic oscillations, revealing the efficacy of the newly developed technique in combustion instability analysis.

2.EXPERIMENTAL SET-UP AND DIAGNOSTICS

The test images are taken from a combustion instability setup in which the methane-air flame, which is stabilized in a non-premixed swirl stabilized burner (IIST-GVS1, see Fig. 1(a)), exhibited naturally excited instabilities under certain operating conditions of the burner. The burner is mounted inside an optically accessible test section of square cross-section (100 mm x 100 mm) and 1000 mm in length. The swirl intensity

(S_M), defined as the ratio of the tangential to the axial airflow momentum, is maintained at 46.7. S_M can, therefore, be varied by independently varying the axial and tangential airflow through the burner. More information about the burner can be found in [4]. Being a non-premixed burner, a lifted flame is observed under these test conditions. A sample time-averaged flame luminosity image is shown in Fig. 1(b). The test data is taken for two different flow Reynolds numbers, 19400 and 29100, which are defined with respect to the inner diameter of the air nozzle and bulk inflow velocity. The air and fuel flow rates are adjusted to achieve a global equivalence ratio (ϕ_g) of 0.9 at the two *Re* conditions.

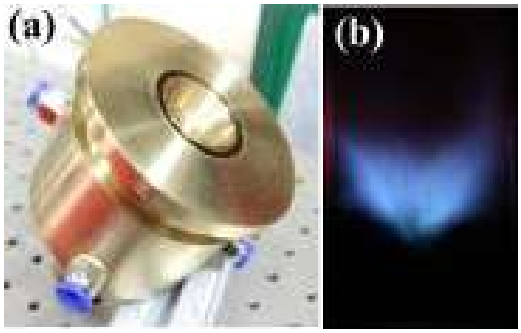

Fig. 1: (a) Photograph of the variable swirl burner (IIST-GVS1) (b) exemplary flame luminosity image

The diagnostic system included acoustic pressure measurements using a transducer (PCB Piezotronics, Model: 103B02; 200 kHz sampling rate, 10 s sampling duration) mounted close to the burner plate in the combustor at the end of an air-cooled probe. Simultaneous measurements of flame luminosity imaging and density gradients (Schlieren) are performed at 2 kHz sampling rates to gather information about the instantaneous changes in the overall flame characteristics and the density gradients present in the approaching fluid flow. Two high-speed cameras from Phantom (Model: v1210 and Miro LAB 3a10) are used for this purpose. Therefore, the high-speed or high framerate (kHz) acquisition provides the transient information of the above flow and flame characteristics.

3. IMAGE POST-PROCESSING

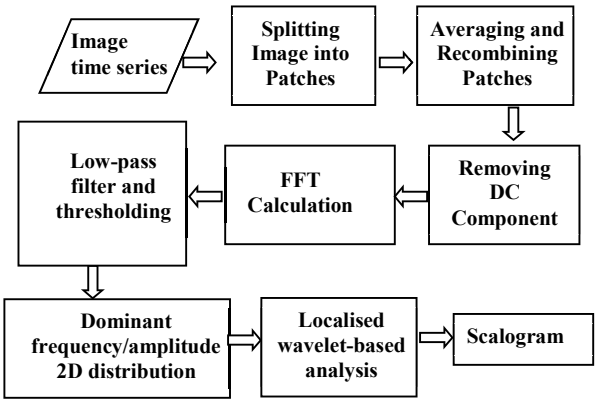

Fig. 2. Digital image processing flow diagram for estimation of the spatial distribution of the dominant frequency, and, the wavelet transforms of localized oscillations from time-series images.

A combined Fourier and Wavelet analysis is applied to the flame luminosity and Schlieren image time series to gain insight into the spatial distribution of oscillations. A post-processing algorithm is developed for the same. The proposed scheme consists of several sub-modules, as shown in the flow diagram in Fig. 2. All the modules of the have been written in Python 3.9.

Fig. 3: Sample flame luminosity image

An exemplary instantaneous flame luminosity image from the burner exit extracted from a high-speed image sequence is shown in Fig. 3. The algorithm employed for estimating the localized intensity oscillation frequency and its amplitude is given in Algorithm 1. A brief description of the different image-processing steps followed is as

follows:

Algorithm 1 FFT Analysis and Visualization

Input: $\{P_i\}_{i=1}^{N}$, a set of N input data points
Output: $\{F_i\}_{i=1}^{M}$, a set of M output frequency distributions
procedure DATAPREPROCESSING
    Load input data: $\{P_i\}_{i=1}^{N}$
    Select time range: $T = [t_{start}, t_{end}]$
    Crop data: $D = \{P_i\}_{i=1}^{N} \cap T$
end procedure
procedure PATCHIFICATION
    Create patches: $Patches = \{P_i\}_{i=1}^{N} \mapsto \{Patches_i\}_{i=1}^{N}$
    Calculate mean of patches: $\{Mean_i\}_{i=1}^{N}$
end procedure
procedure FFT
    Calculate FFT of mean: $\{FFT_i\}_{i=1}^{N}$
    Filter FFT: $\{Filtered_i\}_{i=1}^{N}$
end procedure
procedure FREQUENCYDISTRIBUTION
    Calculate frequency distribution: $\{F_i\}_{i=1}^{M}$
    Sort and arrange data: $\{F_i\}_{i=1}^{M} \mapsto \{Sorted_i\}_{i=1}^{M}$
end procedure
procedure VISUALIZATION
    Plot frequency distribution: $\{Sorted_i\}_{i=1}^{M} \mapsto \{Plot_i\}_{i=1}^{M}$
    Save plots: $\{Plot_i\}_{i=1}^{M} \mapsto \{File_i\}_{i=1}^{M}$
end procedure

Patches Splitting and Recombination after Averaging: -

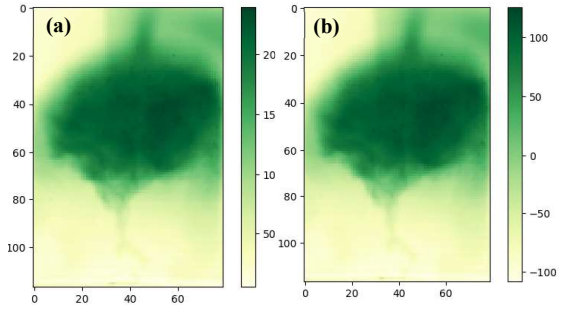

Fig. 4: (a) Image obtained after integrating the average of patches; (b) Image after mean normalization.

Since the Schlieren images are of high resolution, they are split into small image patches (pixel binning) to reduce computational overhead and time. The patch resolution is a user input, with lower values giving higher resolution. Further, for each patch, the average value of the entire patch is calculated and integrated to form pooled images with a lower resolution while preserving the information. A sample image after the process is depicted in Fig. 4(a). Here, the image has been color-mapped to a specific scheme and presented with a false color bar, allowing for a visual representation of pixel intensity.

DC component removal and Fast Fourier Transform (FFT) calculation: -

For each post-integrated image in the sequence, the average of all pixel values is computed and subtracted from each pixel to eliminate the DC component. This process, known as centering the data or mean normalization, helps remove bias in the dataset. The image after mean normalization is shown in Fig. 4(b) in false colors. After applying mean normalization to all images in the series, the FFT is calculated for each patch, spanning the entire integrated image sequence.

Low Pass Filtering (LPF) and Thresholding: -

LP filtering is utilized on the FFT series to eliminate noise, mainly targeting the low-frequency components. Additionally, a thresholding process based on the FFT amplitude filters out frequency components with low amplitudes. This dual approach helps to enhance the quality of the FFT data by reducing noise and focusing on significant frequency components.

Sorting of Dominant Frequencies: -

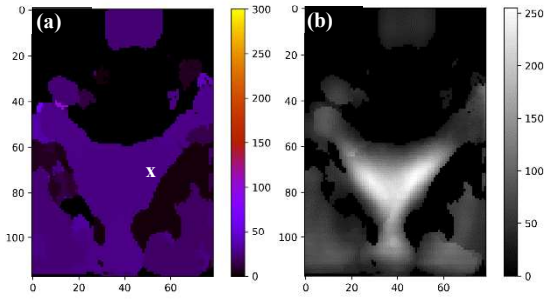

Fig.5: (a) Image displaying all the dominant frequency for each pixel; (b) Corresponding amplitude for each frequency

The frequency values in the FFT array are sorted according to their FFT amplitudes. Subsequently, the highest amplitude value from each sorted FFT array is integrated into an image to visualize the most dominant frequency for each patch. This process allows for the observation of the localized primary frequency components across the image, as illustrated in Fig. 5(a). Further, the 2D

distribution of the amplitude of each dominating frequency is shown in Fig. 5(b).

Wavelet Transform Calculation and Spectrogram: -

From the 2D dominant frequency distribution plot, a specific location of interest is chosen to extract temporal information about the frequencies present. This involves identifying the time duration and the frequencies displayed by the selected pixel. This targeted approach allows for a detailed analysis of the temporal characteristics and frequency components exhibited by the local flow/flame features at the patch under investigation. A wavelet-based approach is followed, and the algorithm for the same is given in Algorithm 2. Further, a scalogram is plotted to display the localized temporal evolution of the dominant frequency, as shown in Fig. 6. The plot clearly shows the existence of an almost steady low-frequency flame intensity oscillation at the selected location of interest marked 'x' in Fig. 5a.

Algorithm 2 Wavelet Analysis of Pixel-Selected Intensity Time Series

1: Input: pl (Pixel location) [User Input]
2: $s = data[:, pl[0], pl[1]]$
3: $t = gen\_time(data.shape[0])$
4: $t = t/fs + init\_time$
5: $sc = gen\_scale(min\_scale, max\_scale)$
6: $c, f = wt(s, sc, wavelet, fs)$
7: Plot scalogram using t, f, and c with 'inferno' colormap
8: Save to file 'calo-' + pl + '.png'

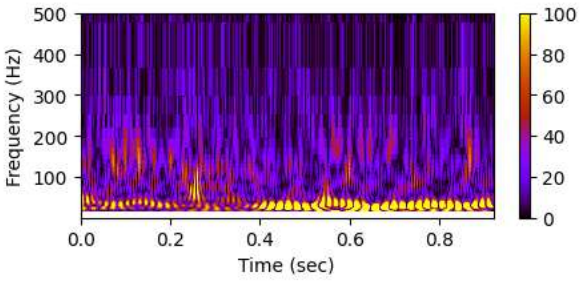

Fig. 6: The scalogram of the pixel of interest marked 'x'(x,y: 50,70) in Fig. 5a).

3. RESULTS

The FFT of the acoustic pressure signal captured from the combustor for the two investigated cases of *Re* = 19400 and 29100 is shown in Fig. 7. for ϕ_g = 0.9. Under the burner's operating condition, the combustor produced self-excited acoustic oscillations with a dominant frequency of approximately 120 Hz and 162 Hz at *Re* = 19400 and 29100, respectively, which is evident in the FFT plot.

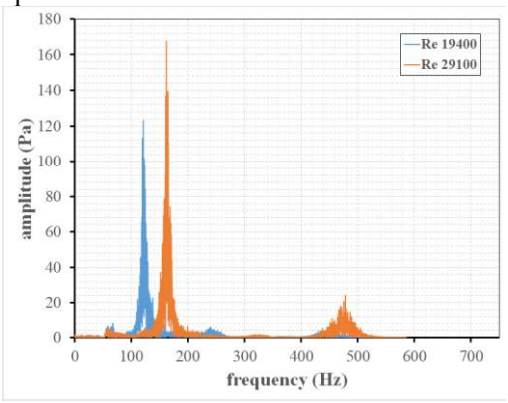

Fig. 7: FFT of the acoustic pressure in the combustor for the two test conditions Re = 19400 and 29100 for a fixed swirl strength of S_M = 46.7 and a ϕ_g = 0.9

Figures 8 and 9 show the output after applying the post-processing techniques on the flame luminosity and Schlieren high-speed image time series for the two *Re* cases discussed above. Here, flame luminosity images give a good impression of the overall flame characteristics, namely the size and shape of the flame, flame stabilization location, and local flame intensity. It captures the overall emissions from reactive species in the flame in the visible region of the electromagnetic spectrum and is an approximate measure of the heat released from the flame. On the other hand, Schlieren imaging gives information about the density gradient in the reactive and non-reactive flowfields in the region of interest (ROI). In the present study, these images provide a good impression of the presence of vortical structures approaching the flame front.

Fig. 8(a) shows an instantaneous and flame luminosity and Schlieren image at *Re* = 19400. The heat release is voluminous, extending close to the exit of the burner. The Schlieren image shows a vortex developing from the exit of the burner at the same instant. The vortex-induced heat release oscillations and the spatial distribution of the corresponding frequency obtained from the FFT of the intensity time series are shown in Fig. 8(b). The plot reveals that a large region of the flame zone is oscillating at almost the same frequency as

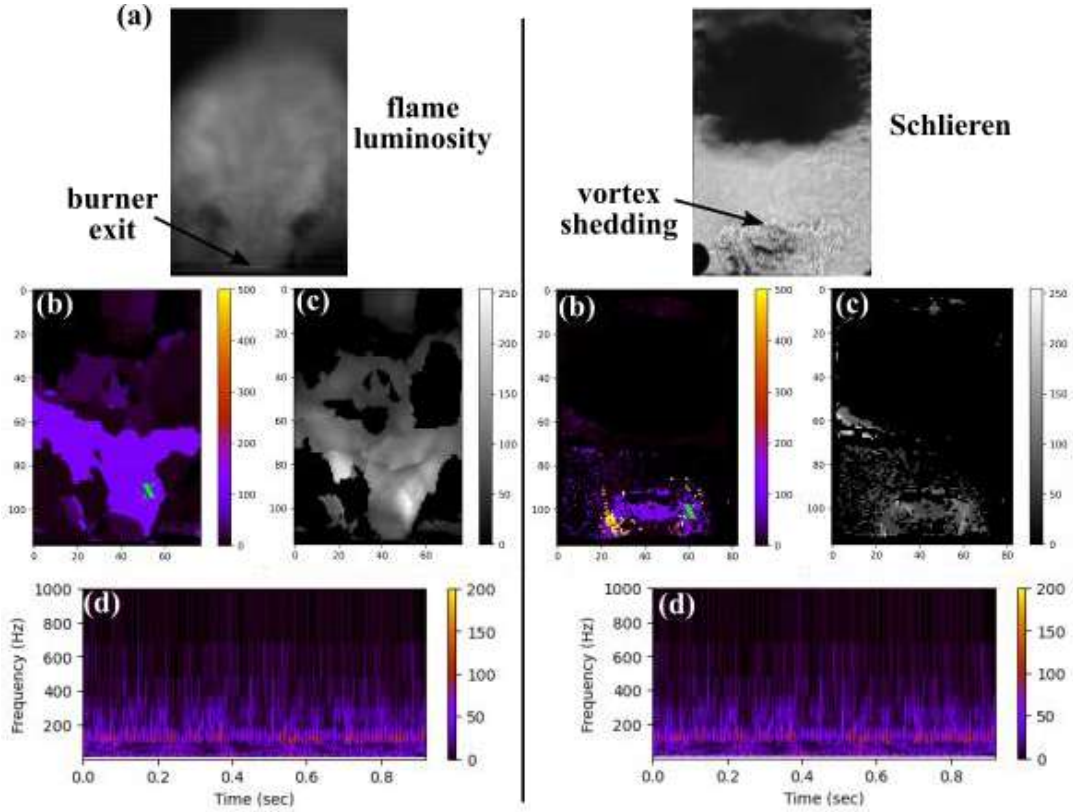

Fig 8: For Re = 19400 and ϕ_g = 0.9 (a) instantaneous flame luminosity (left) and Schlieren image (right) showing vortex shedding from the burner exit (b)2D frequency distribution, (c) corresponding 2D amplitude distribution at the dominant frequency at each location and (d) scalogram of the signal extracted from the yellow 'x' mark in (b).

the acoustic oscillations. However, the region of oscillations and the spatial distribution of the oscillation amplitude (shown in Fig. 8(c)) are not axisymmetric, though the burner is axisymmetric. On the other hand, the localized oscillations and their amplitude in the Schlieren images are almost symmetric. The pronounced oscillations in Schlieren images correspond to the periodic vortex shedding from the burner exit. Wavelet-based analysis is performed at the pixel location marked 'x' in Fig. 8(b) to investigate the temporal development of the flame and vortex shedding frequency. The dominant frequency (~120 Hz) shown in Fig. 8(d) approximately matches the frequency of acoustic pressure, implying that the chamber acoustics most probably induce the vortex shedding, and a close coupling of the acoustic pressure with flame oscillations exists.

Fig. 9(a-d) shows the results for the burner operating condition of *Re* = 29100 and ϕ_g. = 0.9. As in the case of *Re* = 19400, periodic oscillation of the flame intensity and vortex shedding was also observed in the high-speed flame luminosity and Schlieren sequences. However, the 2D frequency distribution of the flame intensity and the oscillation amplitude shown in Fig. 9(b) and 9(c), respectively, is symmetrical with respect to the burner axis. In addition, the vortex shedding frequency distribution is spread over a broader region with a relatively lesser amplitude of oscillation. The scalogram extracted from the location marked 'x' shows that the luminosity oscillations are also very intermittent in nature. The vortex shedding frequency on the other hand is almost aperiodic.

The above results show that the methodology followed is very valuable in the diagnosis of the combustion instability problem. The methodology followed can be used to give a deeper insight into the effect of acoustic oscillations on the 2D distribution of the flame intensity and flow oscillations and their temporal characteristics.

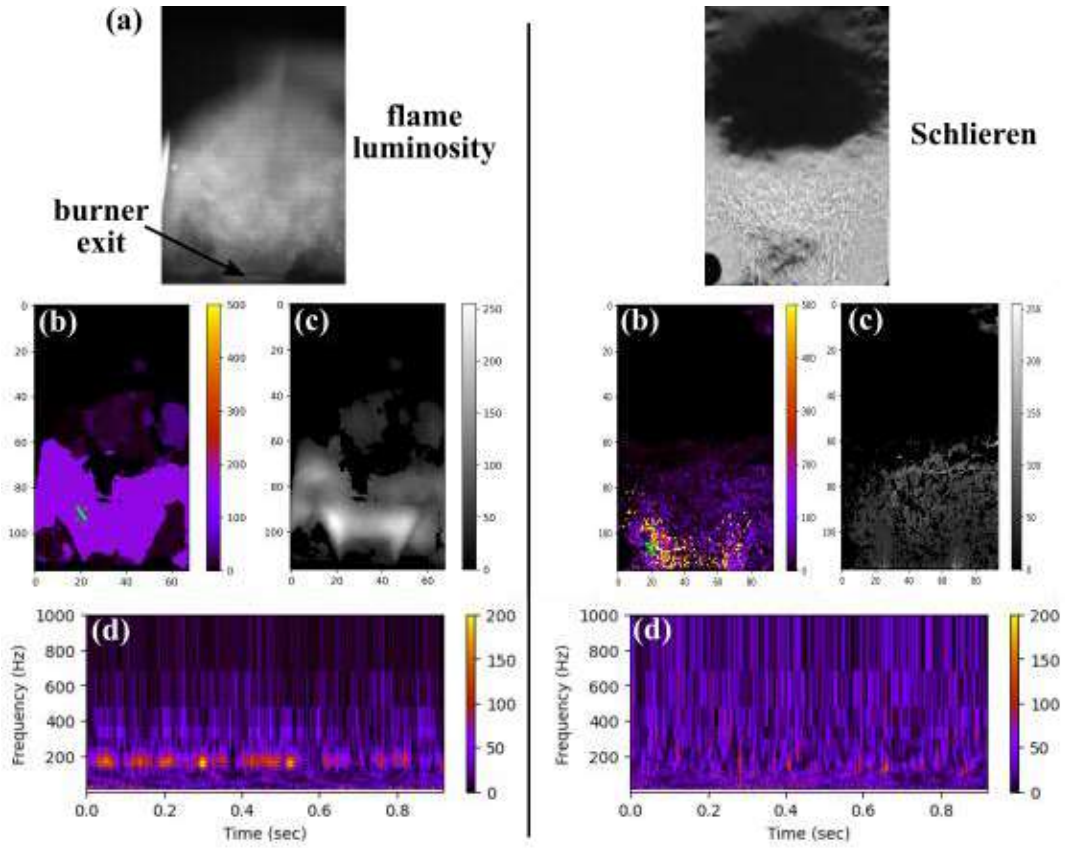

Fig 9: For Re = 29100 and ϕ_g = 0.9 (a) instantaneous flame luminosity (left) and Schlieren image (right) showing vortex shedding from the burner exit (b) 2D frequency distribution, (c) corresponding 2D amplitude distribution at the dominant frequency at each location and (d) scalogram of the signal extracted from the yellow 'x' mark in (b).

4. CONCLUSIONS

The application of digital image processing techniques to get insight into the acoustic instabilities in the combustion systems is reported. The methodology involves a combined Fourier and Wavelet-based analysis on high-speed luminosity and Schlieren image sequences from a non-premixed and swirl stabilized burner. The first part of the image post-processing procedure includes estimating the frequency and amplitude of local intensity oscillations using FFT. The temporal evolution of the dominant frequency at the specific region of interest is then calculated through wavelet-based analysis of the temporal oscillations. A Python-based code is developed to automate the above procedure. The method is applied to swirl burner operating conditions at two Reynolds numbers. At a global equivalence ratio of 0.9, the burner exhibited self-excited oscillations at these flow Reynolds numbers. The results show a close coupling of the combustor acoustic with flame and Schlieren oscillations at low *Re*, whereas the coupling is intermittent at high *Re*. In addition, the 2D dominant frequency and amplitude distribution show an asymmetric excitation of flame intensity at low *Re*, which further attests to the usefulness of the newly developed image processing technique.

REFERENCES

1. S. Candel, "Combustion dynamics and control: Progress and challenges", *Proceedings of the Combustion Institute*. 29 (2002) 1–28.
2. T. Lieuwen, V. Yang, Combustion instabilities in gas turbine engines: Operational Experience, Fundamental Mechanisms, and Modeling, AIAA, Virginia, 2005
3. I. Boxx, C.D. Carter, K.P. Geigle, W. Meier, B.A. – Kumgeh, J. Lewalle, "A spontaneous transition in swirl-stabilized flames".Proceedings of the ASME Turbo Expo (2017), GT2017-64438.
4. Sadanandan, N. (2022) The influence of varying fuel composition and flowfield on turbulent biogas-like flame characteristics, Flow.Turb. Comb., 110 (2023) 689–705.